$$\left(\frac{S-P}{P}\right)\sqrt{\frac{S-P}{S+P}}\,\Bigg]\frac{d\beta}{P} \qquad (A19)$$

$$J^{04} = \frac{2\pi}{B}\int_{-1}^{1}\beta^4\frac{d\beta}{\sqrt{(S+P)(S-P)}} \qquad (A20)$$

$$J^{22} = \frac{\pi}{B}\int_{-1}^{1}\beta^2(1-\beta^2)\left[1-\sqrt{\frac{S-P}{S+P}}\,\right]\frac{d\beta}{P} \qquad (A21)$$

The terms involving square roots can be expressed as elliptic integrals (13) of the first (F) and second (E) kind. Thus, if we substitute

$$\delta^2 = \left(\frac{\alpha_x-\alpha_z}{\alpha_x}\right)\beta^2 \qquad (A22)$$

into Equations (A19) to (A21), the results appear in terms of polynomials and

$$F(\Phi,\kappa) = \int_o^{\delta_1}\frac{d\delta}{\sqrt{1-\kappa^2\delta^2}\,\sqrt{1-\delta^2}} \qquad (A23)$$

$$E(\Phi,\kappa) = \int_o^{\delta_1}\frac{\sqrt{1-\kappa^2\delta^2}}{\sqrt{1-\delta^2}}\,d\delta \qquad (A24)$$

where

$$\delta_1 = \sin\Phi = \left(\frac{\alpha_x-\alpha_z}{\alpha_x}\right)^{1/2} \qquad (A25)$$

$$\kappa^2 = \frac{\alpha_x}{\alpha_y}\left(\frac{\alpha_z-\alpha_y}{\alpha_z-\alpha_x}\right) \qquad (A26)$$

The tedious translation into explicit functions of m and the subsequent regrouping are omitted here. Results are displayed in Equations (27) to (34).

Manuscript received December 23, 1965; revision received April 18, 1966; paper accepted April 19, 1966.

Slip Velocity of Particulate Solids in Vertical Tubes

JENNINGS H. JONES, WALTER G. BRAUN, THOMAS E. DAUBERT and H. DONALD ALLENDORF

Pennsylvania State University, University Park, Pennsylvania

An equation using only easily determined physical properties of particles has been developed for calculating the slip velocity of nonspherical particulate solids falling in fluid media in the intermediate flow range where neither the Stokes nor Newton law applies. The variation in Reynolds numbers covered by this work ranged from 12 to 460. Slip velocities calculated from the equation differed from experimental data by an average deviation of only 3.7% when solids of a wide range of diameters (156 to 1,247 microns), densities (71 to 475 lb./cu. ft.), surface shape factors (0.40 to 0.97), and gases of a wide density range (0.01 to 0.31 lb./cu. ft.) were utilized. Thirty-eight different gas-solid systems were studied.

In any system where solids are to fall through or are to be lifted by fluids a knowledge of the slip velocity of the solids is of great importance. At present there is a definite lack of experimental data in the literature for fluid-solid systems. The present work (2) in the intermediate or transition region between where the Stokes and Newton laws apply has been carried out to develop an accurate equation for slip velocity calculations for both spherical and nonspherical particles.

THEORY

The slip velocity of a single body falling in a fluid is defined as the constant equilibrium velocity attained by the body when the resistance offered by the viscous medium increases to the point where it is equal to the gravitational acceleration force. If the fluid is also stationary and infinite, the slip velocity equals the terminal velocity.

It has been demonstrated experimentally (4) that the resistance φ of a particle in motion involves four quantities: the surface area of the particle A_p, its terminal velocity u_t, and the viscosity μ_f and density ρ_f of the medium through which the particle is flowing. The relationship involved may be expressed by the following equation:

$$\varphi = k_1\,(A_p)^a(u_t)^b(\rho_f)^c(\mu_f)^d \qquad (1)$$

It should be noted that the area used here is the actual surface area of the particle rather than the area of the particle projected on a plane perpendicular to the direction of flow as used by several previous investigators. The actual area was chosen as it is much more readily determined experimentally.

On applying dimensional analysis and substituting the fundamental units of mass M, length L, and time T, this can be expressed as

$$\frac{ML}{T^2} = k_1\,(L^2)^a\left(\frac{L}{T}\right)^b\left(\frac{M}{L^3}\right)^c\left(\frac{M}{LT}\right)^d \qquad (1a)$$

Equating indices of corresponding terms, since the equation must be dimensionally correct, solving for b, and substituting in Equation (1), one obtains

$$\varphi = k_1\,(A_p)^{\frac{b}{2}}(u_t)^b(\rho_f)^{b-1}(\mu_f)^{2-b} \qquad (2)$$

H. Donald Allendorf is with Aerochem Research Laboratories, Inc., Princeton, New Jersey.

The gravitational pull F on the particle can be shown by

$$F = \alpha_v D_p^3 (\rho_s - \rho_f) g \tag{3}$$

When the particle has reached its maximum velocity, or terminal velocity, the resistance φ must equal the gravitational pull F. Thus, by combining Equations (2) and (3) a general relationship for the terminal velocity is obtained:

$$u_t = \frac{k_2 g^{\frac{1}{b}} \alpha_v^{\frac{1}{b}} D_p^{\frac{3}{b}} (\rho_s - \rho_f)^{\frac{1}{b}}}{(A_p)^{\frac{1}{2}} \rho_f^{1-\frac{1}{b}} \mu_f^{\frac{2}{b}-1}} \tag{4}$$

A surface shape factor χ may be incorporated into Equation (4). This may be defined as the ratio of the surface area A_p' of a particle calculated from the volume-surface statistical diameter assuming it to be spherical and the actual surface area A_p of the particle. Thus

$$\chi = \frac{A_p'}{A_p} = \frac{\pi D_p^2}{A_p} \tag{5}$$

On substituting the surface shape factor into Equation (4) one obtains

$$u_t = \frac{k_3 g^{\frac{1}{b}} \alpha_v^{\frac{1}{b}} \chi^{\frac{1}{2}} D_p^{\frac{3}{b}-1} (\rho_s - \rho_f)^{\frac{1}{b}}}{\rho_f^{1-\frac{1}{b}} \mu_f^{\frac{2}{b}-1}} \tag{6}$$

If in Equation (6) b is equal to 1, Stokes' law for small particles moving in streamline motion is obtained. If b is equal to 2, Newton's law for bodies in turbulent motion results.

No sharp boundary exists between streamline and turbulent flow, however, and there is quite an extensive region where neither streamline nor turbulent flow equations apply. For this intermediate region, Allen (*1*) found the value of b to be 3/2 and Equation (6) becomes:

$$u_t = \frac{k_3 g^{\frac{2}{3}} \alpha_v^{\frac{2}{3}} \chi^{\frac{1}{2}} D_p^{\frac{2}{3}} (\rho_s - \rho_f)^{\frac{2}{3}}}{\rho_f^{\frac{1}{3}} \mu_f^{\frac{1}{3}}} \tag{7}$$

In order to determine the terminal velocity of a particle it is necessary to know which of the above equations apply. Thus, Lapple (*8*) presented the following Reynolds number relationship to define the flow regime for a given system:

$$N_{Re} = \frac{D_p \rho_f u_t}{\mu_f} \tag{8}$$

For Stokes' law, the Reynolds number is between 0.0001 and 2.0; for the intermediate range the Reynolds number is between 2.0 and 500; for Newton's law the Reynolds number is between 500 and 200,000.

For those cases where the fluid is not infinite and/or stationary, the constant equilibrium velocity is the slip velocity rather than the terminal velocity. Since the same physical laws govern the two velocities, the foregoing derivations also apply to the slip velocity of the particle.

PREVIOUS WORK

Although there is a lack of experimental data in the literature on the terminal velocity of solids in gaseous media, some data for the fall of solids in liquid media have been reported. Heywood (*5*) and Pettyjohn and Christiansen (*10*) developed relationships for the various flow regions. The latter authors concluded that under streamline flow conditions Stokes' law can be applied to within 2%, and under turbulent flow conditions Newton's law can be applied to within 4%.

Dalla Valle (*4*) presented equations for all regions for both spherical and nonspherical particles incorporating parameters specific to each solid. Korn (*6*) and Lapple (*8*) presented equations for calculating terminal velocities of spherical particles. Leva (*9*) and Zenz and Othmer (*14*) reviewed the several correlations for calculating terminal velocities of spherical and nonspherical particles based on drag coefficient principles. Becker (*3*) proposed a method for the calculation of terminal velocities of nonspherical particles, giving special attention to the intermediate range.

Richardson and Zaki (*11*) while analyzing data from sedimentation and fluidization experiments, found that

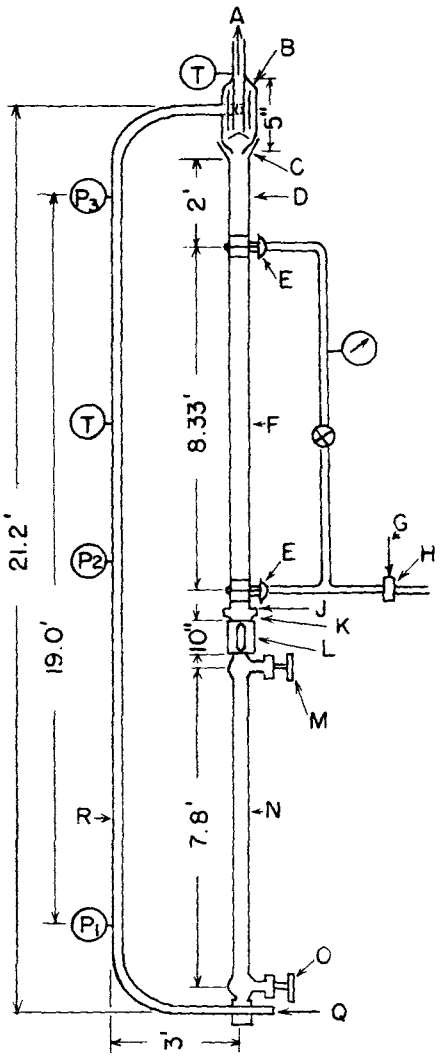

Fig. 1. Slip velocity determination apparatus. A, lift fluid exit. B, cyclone separator (3-in. *D*, steel). C, funnel (6-in. *D*). D, acceleration section (1½-in. *D*, steel). E, quick closing valve. F, slip velocity section (1½-in. *D*, Pyrex). G, air supply to pneumatic valves. H, solenoid valve. J, fluid media injection. K, sampling box. L, sight glass. M, solids rate valve. N, solids standpipe (1-in. *D*, steel). O, solids flow valve. P, pressure tap. Q, lift fluid entrance. R, solids lift line (⅜- to 1-in. *D*, steel). T, thermometer.

the ratio of the slip velocity of a suspension of particles to the terminal velocity of a single particle is a function of the particle Reynolds number, the voidage of the suspension of particles, and the ratio of the particle diameter to the tube diameter. They also showed that for sedimentation experiments the slip velocity and terminal velocities are essentially identical, whereas in the case of fluidization the difference in the logarithms of the terminal velocity and the slip velocity are equal to the ratio of the particle diameter to the tube diameter.

EXPERIMENTAL

Apparatus

A diagram of the apparatus used to determine the slip velocities of solid particles in free fall is shown in Figure 1. The solids flowed from the bottom of the standpipe into the air stream which pneumatically conveyed them through the lift line and into the cyclone which separated the solids and the air. The air exited at the top of the cyclone and the solids fell downward through the bottom of the cyclone into the free-fall section. The gaseous media used for the slip velocity determination was injected at the bottom of the free-fall section and flowed upward and countercurrent to the flow of solid particles. The solids then passed into the solids bed to begin the cycle again.

The solids standpipe served to store the particles and also to provide a bed of solids deep enough to prevent the pressure drop in the lift line from fluidizing the bed. A 1-in. gate valve with the gate partially cut away on the bottom side (to prevent packing of the solids in the valve body) was used to regulate the solids flow. An electric vibrator located above the gate valve insured a steady flow of particles into the air stream.

The slip velocity section was closed off by two fast acting air-to-open Flex-Valves which operated simultaneously. A removable sampling box and a calibrated sight gauge approximately 9/16 in. in diameter was located directly below the sampling box. A gate valve, modified in the same manner as the solids flow valve and fitted with a fine screen to allow gases to pass upward, was located below this sight gauge.

Source of Materials

The glass beads were obtained from the Minnesota Mining and Manufacturing Company as their Scotchlite glass beads in grade numbers of 11, 9, and 6. The fused alumina was obtained from the General Abrasive Company as their white Lionite grade in size numbers 36, 60, and 100. The zircon silica was obtained from the Carborundum Company and was supplied in the 40 to 60 mesh size range. The steel shots A and B were obtained from stocks in this laboratory and their origin is not known. Steel shot C was obtained from Steel Shot Producers, Inc., as their No. 70 Tru-Steel Shot. Steel shot D was obtained from the Abrasives Metals Company as their S-170 Superior X Shot. The poppy seeds were obtained from a local bakery. The argon was obtained from the Linde Air Products Company and was said to have a purity of 99.996 vol. %. The carbon dioxide was obtained from the Linde Air Products Company and was said to have a purity of 99.0 vol. %. The Freon-12 (dichlorodifluoromethane) was obtained from the Matheson Company, Inc., and was said to have a minimum purity of 97.0 vol. %. The helium was obtained from the Linde Air Products Company and was said to have a purity of 99.6 vol. %.

Procedures

Determination of Solid Particle Properties

Sizing the Solid Particles. The solid particles were separated into their size ranges with 8-in. diameter Tyler Standard Scale Testing Sieves and a Ro-Tap Testing Sieve Shaker. A portion of the solid particles was placed on the top screen, and the sieve assembly was shaken for approximately 15 min. The solid particles were then separated according to their screen sizes. This process was repeated until a sufficient quantity of solids of the size desired was obtained.

Solid Particle Density. The density of the solid particles ρ_s was determined by the displacement method. A known volume of acetone was pipetted into a 250-cc. Cassia volumetric flask and the combined weight of the flask and acetone was obtained. Solid particles were added to the flask until the level of acetone reached the calibrated portion in the neck of the Cassia flask and the combined weight of the acetone, solids, and flask was obtained. The solids density was calculated as follows:

$$\rho_s = \frac{(\text{wt. of solids} + \text{acetone} + \text{flask}) - (\text{wt. of acetone} + \text{flask})}{\text{total volume} - \text{volume of acetone used}}$$

Three or four determinations were made for each solid and an average density was obtained.

Solids Bed Density. The solids bed density ρ_b was determined by slowly pouring the solid particles into a preweighed 250-cc. graduated cylinder. The graduated cylinder was hand-vibrated as the solids were added in order to obtain uniform settling. The level of the solids in the graduated cylinder was recorded and a combined weight of the solids and cylinder obtained. The bed density was obtained from the weight and volume of solid particles added to the cylinder.

Particle Diameter Determinations. The diameter of the solid particles was measured with a Spencer microscope with powers of 20× and 120× and a fixed scale micrometer eye piece. At least two hundred measurements were made for each solid used. A table was made which listed the number of the particles n at each diameter D measured and a statistical diameter was obtained as follows:

$$D_p = \frac{\Sigma\, nD^3}{\Sigma\, nD^2} \tag{9}$$

TABLE 1. PHYSICAL PROPERTIES OF THE SOLIDS

Solids	Particle diameter D_p, microns	D_p, ft. × 10^4	D_m, microns	s, microns	n	Solids density ρ_s, lb./cu. ft.	Solids bed density ρ_b, lb./cu. ft.	Surface area A_o, sq. ft./cu. ft.	Surface shape factor χ
Glass beads No. 111	156	5.12	151	20.4	241	154	96.0	12,100	0.967
Glass beads No. 109	349	11.5	333	28.8	254	158	100	5,510	0.947
Glass beads No. 106	578	19.0	570	45.8	251	156	98.5	3,560	0.887
Fused alumina No. 100	201	6.59	182	30.8	213	243	126	20,200	0.450
Fused alumina No. 60	453	14.9	438	57.6	226	247	133	9,410	0.429
Fused alumina No. 36	740	24.3	732	61.0	263	243	135	6,120	0.403
Zircon silica No. 1	561	18.4	549	50.7	272	217	133	4,230	0.769
Zircon silica No. 2	382	12.5	369	40.4	305	208	132	6,270	0.763
Steel shot A	490	16.1	482	43.9	253	472	290	4,750	0.785
Steel shot B	509	16.7	498	53.6	261	462	292	4,320	0.830
Steel shot C_1	273	8.95	269	21.6	254	474	286	6,950	0.964
Steel shot C_2	322	10.6	310	27.3	232	475	292	6,340	0.895
Steel shot D_1	765	25.1	760	38.5	243	453	292	3,200	0.747
Steel shot D_2	660	21.6	658	38.8	258	452	286	3,560	0.777
Poppy seeds	1,247	40.9	1,227	139	254	71.1	42.7	3,100	0.472

In Equation (9) D_p is the mean volume-surface diameter (*4*). This statistical diameter was chosen for correlational purposes because it was based on specific surface per unit volume and could be directly related to the surface area of the solid particles determined as outlined below.

Table 1 compares this diameter with the mean diameter and the standard deviation of the diameter from the mean.

Solids Surface Area Determination. The surface area of the solid particle A_o was determined by permeability principles as explained by Sullivan and Hertel (*12*). The apparatus was designed by Lakhanpal et al. (*7*). Although the areas determined by this method may not be the absolute values, there is no known method for determining them. However, the permeability method gave values for the surface areas of the various particles which can be directly used to determine the shape factors for the particles, thus making it unnecessary to determine the absolute values of the surface area. The shape factor was determined by applying Equation (5) in the following form:

$$\chi = \frac{\pi D_p^2}{A_p} = \frac{\pi D_p^2}{\frac{\pi}{6} D_p^3 A_o} = \frac{6}{D_p A_o} \qquad (10)$$

The properties of the solids determined by the methods described are also given in Table 1.

Solids Rate Determination. The solids rate was determined by timing the accumulation of the solid particles as they filled the calibrated sight gauge on closing the solids rate valve. The accumulation in a certain period of time was measured and was converted to mass flow per unit time.

Slip Velocity Determinations. The gaseous media (air, helium, carbon dioxide, argon, and Freon-12) in which the slip velocity was determined were injected into the free-fall section at the point indicated in Figure 1. The flow rate of the gaseous media was measured by means of an orifice meter previously calibrated against a low pressure orifice prover. The solid particles were circulated until steady state was obtained and the solids rate was determined.

The pair of Flex-Valves was then closed simultaneously in order to trap the solids present in the slip velocity section. The trapped solids then were dropped into the sampling box by opening the lower Flex-Valve while keeping the top Flex-Valve closed. The solids were caught in the sampling box on a preweighed thin-wall aluminum dish. The weight of the trapped solids was obtained with an analytical balance. The slip velocity was obtained by calculating the actual downward velocity of the solid particles and adding the countercurrent velocity of the fluid media.

Several such determinations were made on each type of solid particle at various solids rates and gas velocities.

$$u_s = u_f + u_p \qquad (11)$$

The velocity determined by Equation (11) was the actual slip velocity of the particle, because the voidage in all cases exceeded 0.995 and was in most cases near 0.999, thus approximating a single particle and essentially negating effects of particle interactions.

The length of the acceleration section was too short to allow solids particles with actual slip velocities in excess of 7 ft./sec. to attain this velocity without the aid of the countercurrent gas. The apparent slip velocity increased with increasing gas velocity until the actual slip velocity was reached, after which it held constant with further increase in gas velocity.

Static electricity was encountered in the apparatus when small-diameter solid particles were used (glass beads No. 111 and fused alumina No. 100). In such cases some of the solid particles were attracted to the sides of the Pyrex glass pipe in the slip velocity section causing an error in the slip velocity determinations. Intermittent flow and eventual solid-flow stoppage was also caused by the attraction of the solid particles to the sides of the cyclone. These problems were eliminated entirely by passing the air through a bottle of water before it entered the determination section. Such a procedure increased the relative humidity of the air from 21 to 45%.

RESULTS AND DISCUSSION

Experimental Data

The slip velocities of the solid particles as determined in this work for several fluid media are presented in Table 2.*

In some instances the gas temperature varied slightly when a series of determinations on a particular solid was carried out. In such cases, however, the temperature effect was neglected, since the error introduced in slip velocity was always less than 0.5% which was within the experimental accuracy.

In all cases the deviations in the values found for the slip velocity were well within the range expected for experimental error. The maximum deviation from the average slip velocity for any solid was 5.4% (glass beads No. 111). Such a deviation amounted to only 0.2 ft./sec. from the average slip velocity of 3.7 ft./sec. Ninety per-

* Complete data (Tables 6 to 20) have been deposited as document 8989 with the American Documentation Institute, Photoduplication Service, Library of Congress, Washington 25, D. C., and may be obtained for $2.50 for photoprints or $1.75 for 35-mm. microfilm.

TABLE 2. EXPERIMENTAL AND CALCULATED SLIP VELOCITIES

Gas	Slip velocities, ft./sec. Air		Carbon dioxide		Helium		Argon		Freon-12	
Solids	Experimental	Calculated	Experimental	Calculated	Experimental	Calculated	Experimental	Calculated	Experimental	Calculated
Glass beads No. 111	3.7	3.7	—	—	—	—	—	—	—	—
Glass beads No. 109	8.6	8.4	8.3	7.8	14.7	15.6	7.4	7.1	6.5	6.0
Glass beads No. 106	13.3	13.0	12.4	12.1	24.4	24.3	11.7	11.0	8.2	9.3
Fused alumina No. 100	4.0	3.7	—	—	—	—	—	—	—	—
Fused alumina No. 60	7.8	8.4	8.0	7.8	14.6	15.6	7.4	7.1	—	—
Fused alumina No. 36	12.7	13.0	11.8	12.2	—	—	11.0	11.0	—	—
Zircon silica No. 1	13.9	14.4	13.0	13.4	—	—	12.4	12.1	—	—
Zircon silica No. 2	9.3	9.2	9.4	8.6	17.1	17.3	8.4	7.8	—	—
Steel shot A	21.8	21.3	—	—	—	—	17.6	17.9	—	—
Steel shot B	22.2	22.9	—	—	—	—	19.1	19.4	—	—
Steel shot C_1	13.3	13.6	12.7	12.7	—	—	11.8	11.5	10.0	9.7
Steel shot C_2	15.0	15.2	—	—	—	—	—	—	—	—
Steel shot D_1	30.3	31.2	—	—	—	—	—	—	—	—
Steel shot D_2	27.6	27.8	—	—	—	—	—	—	—	—
Poppy seeds	11.7	10.9	—	—	—	—	—	—	—	—

Values were calculated from Equation (13).

cent of the gas-solid systems investigated had a deviation from the average slip velocity of 3.5% or less.

When the gas velocity was increased it had the same effect as increasing the length of the acceleration section and an increase in the slip velocity was observed. When the gas velocity was increased further, a point was reached where the solid particles attained their slip velocity before entering the determination section, and any further increase in the gas velocity had no appreciable effect on the slip velocities. However, when the gas velocity approached to within 0.5 to 1.0 ft./sec. of the slip velocity, it was noted in most cases that the slip velocities obtained were lower than the true values. In this range there was a large holdup of solids in the determination section and the solid particles collided with each other and with the wall of the tube, thus reducing their velocities.

Slip Velocity Correlation. The Reynolds number of the solid particles was calculated in each fluid studied by means of Equation (8). Based on slip velocity it varied from 12 to 460. By assuming a single particle falling in a finite media, Equation (6) may be written in terms of slip velocity as follows:

$$u_s = k_4 \frac{\chi^c D_p^{\left(\frac{3}{b}-1\right)} (\rho_s - \rho_f)^{\frac{1}{b}}}{\rho_f^{\left(1-\frac{1}{b}\right)} \mu_f^{\left(\frac{2}{b}-1\right)}} \qquad (12)$$

The values of the constant k_4 and the exponents c and b were determined by substituting the experimental values of the slip velocities and the physical properties of the particles and fluids into Equation (12) and by determining a best fit of the data by simultaneous solution of various combinations of the equations.

Equation (13) results:

$$u_s = \frac{2.40\ (\rho_s - \rho_f)^{0.673} (D_p)^{1.020} (\chi)^{0.7}}{(\rho_f)^{0.327} (\mu_f)^{0.347}} \qquad (13)$$

In the above equation the volume factor which appeared in Equation (6) was not considered, because the shape factor χ as calculated incorporated the volume factor. The combination of the volume factor and shape factor accounts for the difference between the theoretical exponent of the shape factor (0.5) and the actual value obtained (0.7).

The gravitational constant g was not included in Equation (13) since there was no way to check this value experimentally. However, it can be incorporated in the equation by simply changing the constant (2.40) of Equation (13).

As stated previously, Allen (*1*) found the value of b in Equation (6) to equal 1.5 for the intermediate range. In the present investigation the value of b determined separately for each solid-gas system varied from 1.43 to 1.54. In the correlation an average value of 1.485 gave the best fit to the data.

As shown in Table 2, Equation (13) is in close agreement with the experimental values obtained for slip velocities. With the exception of one value, the maximum deviation of the slip velocities calculated from this equation was only 8.5% from the experimental values, while the average deviation was only 3.7%. The single exception shown was for glass beads No. 106 when using Freon-12 as the gaseous medium; in this case the deviation was 13.4%. It is believed that this deviation is due to experimental error but exactly where the error was introduced is not known.

Although it would have been interesting and useful to test the correlation of Richardson and Zaki concerning the effect of particle to tube diameter on the relation between slip velocity and actual terminal velocity, this could not be done as all experiments were carried out in the same tube. Furthermore, except for one system the diameter ratio varied only from 0.004 to 0.020. Thus, by assuming the Richardson and Zaki postulation to be correct, the slip velocity data of this work approached the actual terminal velocity of the solids within less than 5% in all cases.

ACKNOWLEDGMENT

The authors express their appreciation to R. A. Rusk of this laboratory for his invaluable assistance.

NOTATION

A_o = surface area of solid particles, sq.ft./cu.ft.
A_p = actual surface area of a particle, sq.ft.
A_p' = surface area of a particle calculated from a statistical diameter by assuming a sphere, sq.ft.
b = exponent
c = exponent
D = diameter of particle, ft.
D_m = mean diameter of particles, microns
D_p = statistical diameter of particles based on specific surface per unit volume, ft.
F = gravitational pull on particles, (lb.)(ft.)/sec.^{2}
g = local gravitational constant, ft./sec.^{2}
k_1, k_2, k_3, k_4 = constants
n = number of particles of any particular group
s = standard deviation of particle diameter from mean, microns
u_f = velocity of fluid media in the slip velocity section, ft./sec.
u_p = velocity of solid particles, ft./sec.
u_s = slip velocity of solid particles, ft./sec.
u_t = terminal velocity of solid particles, ft./sec.

Greek Letters

α_v = volume shape factor, dimensionless
μ_f = viscosity of fluid media, lb./(ft.)(sec.)
ρ_b = bed density of solids, lb./cu.ft.
ρ_f = density of fluid media, lb./cu.ft.
ρ_s = density of solids, lb./cu.ft.
φ = resistance of a particle in motion, (lb.)(ft.)/sec.^{2}
χ = surface shape factor of solid particles, dimensionless

LITERATURE CITED

1. Allen, H. S., *Phil. Mag.*, 1, 323 (1900).
2. Allendorf, H. D., M.S. thesis, Pennsylvania State Univ., University Park (1960).
3. Becker, H. A., *Can. J. Chem. Eng.*, 37, 85 (1959).
4. Dalla Valle, J. M., "Micromeritics," Pitman, New York (1943).
5. Heywood, Harold, *J. Imp. Coll. Chem. Eng. Soc.*, 4, 17 (1948).
6. Korn, A. H., *Chem. Eng.*, 58, No. 11, 178 (1951).
7. Lakhanpal, M. L., V. D. Anand, and B. R. Puri, *Nature*, 176, 692 (1955).
8. Lapple, C. E., "Chemical Engineers' Handbook," p. 1019, McGraw-Hill, New York (1950).
9. Leva, Max, "Fluidization," McGraw-Hill, New York (1959).
10. Pettyjohn, E. S., and E. B. Christiansen, *Chem. Eng. Progr.*, 44, 157 (1948).
11. Richardson, J. F., and W. N. Zaki, *Trans. Inst. Chem. Engrs.*, 32, 35 (1954).
12. Sullivan, R. R., and K. L. Hertell, *Advan. Colloid Sci.*, 1, 37 (1942).
13. Wadell, Hakon, *J. Franklin Inst.*, 217, 459 (1934).
14. Zenz, F. A., and D. F. Othmer, "Fluidization and Fluid-Particle Systems," Reinhold, New York (1960).

Manuscript received August 18, 1965; revision received March 14, 1966; paper accepted March 14, 1966.